DOI: 10.36137/2030E

INSTYTUT KOLEJNICTWA

Railway Reports – Issue 204 (September 2025) ISSN 0552-2145 (print) ISSN 2544-9451 (on-line)

Transition Curves for High-Speed Railways

Władysław KOC[1]

Summary

This paper focuses on conditions for the use of transition curves on high-speed railways. The Technical Specifications for Interoperability (TSI), relating to the "Infrastructure" subsystem of the EU railway system, leave a large margin of discretion in this regard (delegating final resolution of a given problem to national regulations). Based on the applicable EU and national rules, acceptable values for the kinematic parameters that should correspond to the design of transition curves have been proposed. A number of cases were considered, setting minimum values for horizontal curve radii and lengths of transition curves, depending on train speed and cant on the curve. The transition curves that would likely be the most representative from the point of view of high-speed railways were selected: the clothoid, the Bloss curve and a new curve with a smoothed curvature at the end section. Guided by previously established principles, the parameters of the test geometric layouts, which were the subject of comparative analysis, were determined. The analysis showed that smooth transition curves (such as the Bloss curve) cause problems with the shape of the track axis at the initial section; this applies to both horizontal ordinates and gradient due to cant ordinates. For this reason, there have been doubts about the applicability of these curves on conventional railways. On high-speed railways, the constraints of shaping the initial section may be multiplied by the much larger radii of horizontal curves and lengths of transition curves adopted. As such, they do not correspond to the conditions found on these railways. These conditions are undoubtedly met by a clothoid transition curve, but the proposed new form of the curve, which provides a smoother transition to a circular curve on its end section, seems more favourable.

Keywords: high-speed railways, transition curves, kinematic parameters, comparative analysis of test layouts, selection of the most favourable solution

1. Introduction

Many publications on *high-speed railways* (HSR) are descriptive in nature – they deal with general issues, presenting the situation in different countries and mainly addressing selected economic and social considerations. Of course, there are also numerous sources dealing with technical issues, such as railway line design, e.g. [6, 7, 9, 15, 22, 24, 25] or railway turnouts, e.g. [17, 23].

In Poland, where rail transport has long played a crucial role, a functioning high-speed railway system is yet to be established. The relevant work on this issue was very advanced at one point, with the Railway Research Institute in Warsaw playing a leading role; certain government decisions had even been made. The scale of Polish achievements in this matter is best illustrated by a summary study [8]. After several years, the problem has resurfaced and the concept of building high-speed railways is gaining more and more supporters. This is related to the proposal to establish the Solidarity Transport Hub, a major air transport hub planned to be situated near Łódź.

Following Poland's accession to the European Union in 2004, efforts began in many areas to bring Polish regulations into line with EU requirements. This also applied to railways, where relevant legal regulations were developed in the form of Technical Specifications for Interoperability (TSI) and were transposed into Polish legislation. One example is the first version of the Technical Standards [20] developed in 2009, which directly referred to the Technical Specification for Interoperability relating to the "Infrastructure" subsystem of the trans-European conventional rail system CR INF TSI [3] (which at that time still had the status of a working document, not approved by a decision of the Commission of the European Communities). The Technical Specification

[1] Ph.D. D.Sc. Eng. Prof.; Gdańsk University of Technology, Department of Transportation Engineering; e-mail: kocwl@pg.edu.pl.

for Interoperability relating to the infrastructure subsystem of the trans-European high-speed rail system, TSI HS INF [2], adopted slightly earlier, could only apply in Poland to modernised lines rated for travel speeds of 200 km/h (i.e. classified as category II HS lines). The year 2014 saw the release of a *Commission Regulation* [4] that covered TSI issues relating to the entire infrastructure subsystem (i.e. both conventional and high-speed railways). As of 1 January 2015, regulation [4] replaced regulation [2], which was still in force for some time for ongoing projects.

It seems worthwhile to examine what impact the new conditions have had on the design process of track geometric layouts. This mainly concerns the accepted limit values for kinematic parameters. In this respect, the Technical Specifications for Interoperability introduce certain, sometimes quite significant, modifications. Particular attention should be given to those issues that are dealt with in a limited way in the TSI. This is the case with transition curves, for which the new design rules leave considerable discretion. This article addresses precisely the issue of considerations for transition curves on high-speed railways.

2. Permissible values for kinematic parameters

The permissible values of kinematic parameters form the basis for designing the track geometric layout for the assumed train speed, i.e. determining the radii of circular curves, the cant values on curves and the lengths of transition curves (and cant ramps). These values are defined in the regulations [4], which, however, do not cover all the required parameters. Therefore, when designing transition curves, the provisions of applicable national regulations must also be considered [21].

2.1. Track cant and cant deficiency

The regulations [4] assume a maximum *design cant* of $D_0 = 180$ mm for both ballasted and ballastless track. In the Polish Technical Standards [21], the permissible cant value (recommended and normal) for mainline tracks is 150 mm.

Furthermore, both regulations [4] and [21] formally depart from the commonly used term "unbalanced lateral acceleration" and introduce the concept of "cant deficiency". Cant deficiency is the difference (expressed in millimetres) between the applied cant on the track and the equilibrium cant for the vehicle at the particular speed. This is undoubtedly a nod to railway history, but it can be seen as a departure from the basic laws of physics, which state that travelling at a certain speed on a curved track with a cant generates a certain amount of lateral acceleration. The new solution can, of course, be accepted because of the ease of converting the cant deficiency into unbalanced lateral acceleration (taking into account the track gauge). The following formula applies:

$$a_m = \frac{g}{s} I \tag{1}$$

where:

a_m – unbalanced acceleration on a circular curve in m/s^2,
I – cant deficiency in mm,
s – wheel track gauge in mm,
g – acceleration due to gravity ($g = 9.81$ m/s^2).

If the object of our interest is high-speed railways, i.e. essentially railway lines for speeds $V > 250$ km/h, then – when operating rolling stock compliant with the "Locomotives and Passengers TSI" [5] – the normal limit I_{lim} in the interval $250 < V \leq 300$ km/h, as per the regulations [4], is 153 mm. As a normal track gauge (and thus $s \approx 1500$ mm) is used on HSR lines, this corresponds to a permissible unbalanced lateral acceleration value of $a_{per} = 1.00$ m/s^2. For $V > 300$ km/h, the value $I_{lim} = 100$ mm, which corresponds to $a_{per} = 0.65$ m/s^2.

In Technical Standards [21], $I_{per} = 110$ mm (i.e. $a_{per} = 0.72$ m/s^2) is given as the recommended permissible value, and $I_{per} = 130$ mm (i.e. $a_{per} = 0.85$ m/s^2) as the normal permissible value.

2.2. Increase in unbalanced lateral acceleration

The regulations [4] introduce the concept of "abrupt change of cant deficiency", but this is not permitted for speeds above 230 km/h. The issue of transition curves has been completely ignored here; in fact, a similar approach was used in regulations [2, 3]. In this situation, it seems that the resolution of this issue has been left to national regulations.

The Technical Standards [21] developed in Poland refer directly to regulation [4]; they state that the value of abrupt change of cant deficiency should be checked for track layouts with abrupt changes of track curvature. However, they do not specify the permissible value of unbalanced lateral acceleration on transition curves.

Notably, the permissible acceleration increase rate takes on a wide range of values in different countries: $\psi_{per} = 0.15$–0.85 m/s^3 [1]. In this situation, it should be assumed that regulation [18] continues to apply in Poland, which specifies the following permissible value of unbalanced lateral acceleration increase on

individual transition curves (for newly constructed lines and well as existing lines with no superstructure changes): $\psi_{per} = 0.5$ m/s^3.

2.3. Rolling stock wheel lift velocity on the gradient due to cant

The question of the rolling stock wheel lift velocity on the gradient due to cant for high-speed railways does not appear in regulation [4]. It is believed that this issue has been left to be resolved in national regulations. However, in regulation [3] for conventional railways, this parameter has been taken into account – the concept of "rate of change of cant as a function of time" has been introduced. For rolling stock not equipped with a body tilting system, a value of max dD/dt = 70 mm/s was established for all line categories, indicating the possibility of increasing it to max dD/dt = 85 mm/s in certain situations.

In Poland, the Technical Standards [21] retained the notion of dD/dt from regulation [3], but did not adopt the findings presented therein. The following permissible values were distinguished:

- recommended: dD/dt = 35 mm/s,
- normal: dD/dt = 50 mm/s,
- for curvilinear gradients due to cant: dD/dt = 55 mm/s.

2.4. Adoption of kinematic parameter values for the design of transition curves on HSR

As shown by the findings concerning cant and cant deficiency, the conditions for designing a circular curve (i.e., determining the values of the curve radius and cant) for the HSR are clearly established. The following condition must be met:

$$I = 11.8\frac{V_{\max}^2}{R} - D_0 \le I_{per} \qquad (2)$$

where:

D_0 – cant value in mm,
V – train speed in km/h,
R – circular curve radius in m,
I_{per} – permissible cant deficiency in mm.

This article focuses on the design conditions for transition curves. The aim was to ensure that these curves were not too long. In order to do this, the cant values used had to be limited, leading to the need for larger radii of circular curves. It was therefore considered most advantageous to adopt a cant deficiency limit value of I_{lim} = 100 mm. In regulation [4], this applies for speeds V > 300 km/h; the I_{lim} = 153 mm given there for 250 < $V \le$ 300 km/h appears to be an overestimate.

The permissible acceleration increase rate is one of the parameters determining the length of the transition curve. For large circular curve radii, however, it plays a secondary role; the regulations [2–4, 21] do not take this parameter into account. As such, a value of $\psi_{per} = 0.5$ m/s^3, given in the Polish Regulation [18], was adopted for the calculations.

The permissible value of the rolling stock wheel lift velocity on the gradient due to cant, defined in regulation [4] as the rate of change of cant as a function of time, is usually the basic parameter determining the length of the transition curve (and gradient due to cant). Regulation [4] sets a value of $(dD/dt)_{per}$ = 70 mm/s, which deviates significantly (upwards) from the values used so far. For the purpose of this article, it was decided to reduce this value slightly in order to increase driving comfort; the value recommended in the Polish Technical Standards [21] – as a normal acceptable value – $(dD/dt)_{per}$ = 50 mm/s was adopted. It was assumed that it is also valid for curvilinear gradients due to cant.

3. Minimum horizontal curve radii and lengths of transition curves

For a given running speed, the minimum radii of horizontal curves and the lengths of transition curves result from the adopted cant value on the curve. In the analysis carried out, the permissible values of the kinematic parameters adopted in this article were applied. A number of cases were considered for different speeds between 250 and 350 km/h and cant ranging from 60 mm to 180 mm.

The minimum radius of the horizontal curve can be determined using condition (2). Assuming I_{lim} = 100 mm, the graphs shown in Figure 1 would be obtained.

As can be seen, the values of $R_{\min}$ increase with increasing speed V and decrease with increasing cant D_0 (which in itself is obvious). For example, for V = 250 km/h and D_0 = 60 mm, one gets $R_{\min}$ = 4,650 m and for D_0 = 180 mm it is $R_{\min}$ = 2,650 m. Conversely, V = 350 km/h gives the following: with D_0 = 60 mm – $R_{\min}$ = 9,100 m, with D_0 = 180 mm – R_{min} = 5,200 m. In design practice, intermediate cant values are usually adopted, and the horizontal curve radii used are usually greater than the R_{min} values obtained from calculations.

From the point of view of the subject of this article, it will be particularly important to determine the minimum lengths of the transition curves. Formally, these lengths are derived from the requirement not to exceed the permissible values of the increment of

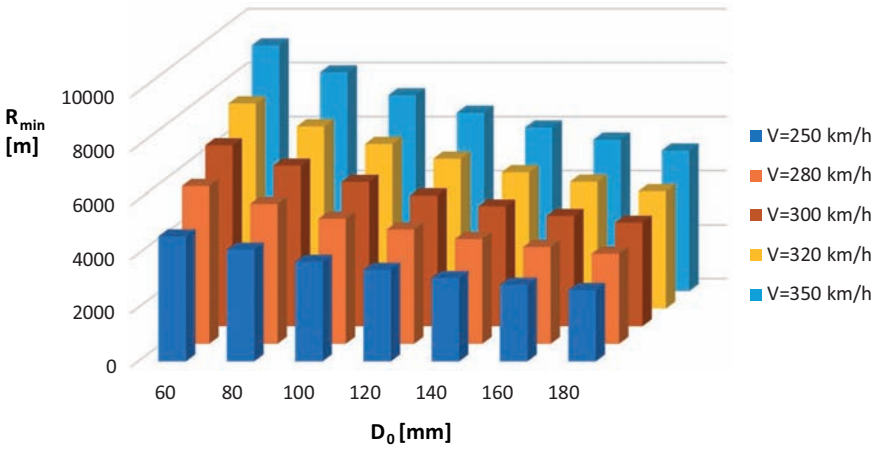

Fig. 1. Graphs of the minimum horizontal curve radius R_{min} depending on the train speed V and cant D_0 on the curve [author's own elaboration]

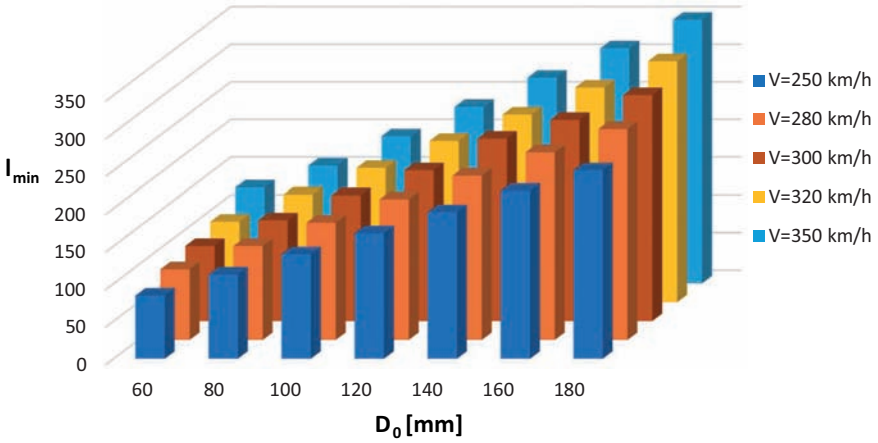

Fig. 2. Graphs of the minimum length of the transition curve l_{min} as a function of train speed V and cant D_0 on the curve [author's own elaboration]

unbalanced acceleration ψ_{per} and the rate of change of cant $(dD/dt)_{per}$. However, computational practice shows that only the latter condition, related to the rolling stock wheel lift velocity on the gradient due to cant, is relevant. So, as with the determination of R_{min}, the *cant* D_0 on the curve plays a decisive role here.

In traffic engineering, the most common form of transition curve is the clothoid (the third degree parabola, which is a simplification of the clothoid, is still used on conventional railway lines; with the current computational possibilities, this is no longer justified). The curvature graph along the length of the clothoid is linear, and the gradient due to cant (if any) is rectilinear. The minimum length of the transition curve resulst from the following formula:

$$l_{\min} = \frac{D_0 V}{3.6\left(\frac{dD}{dt}\right)_{per}} \tag{3}$$

The graphs shown in Figure 2 were obtained for a clothoid transition curve at $(dD/dt)_{per} = 50$ mm/s.

As can be seen, the values of l_{min} increase with increasing speed V and cant D_0. For example, for $V = 250$ km/h and $D_0 = 60$ mm, one gets $l_{min} = 70$ m and for $D_0 = 180$ mm it is $l_{min} = 250$ m. Conversely, $V = 350$ km/h gives the following: with $D_0 = 60$ mm – $l_{min} = 117$ m, with $D_0 = 180$ mm – $l_{min} = 350$ m. The range of minimum transition curve lengths shown is therefore very wide. In design practice, values significantly greater than the minimum are usually adopted. The upper limit is related to problems of performance practice, i.e. the elevation of the gradient due to cant, especially at its initial section. This will be discussed later in this article.

4. Transition curves used

In the analysis carried out, it was first necessary to select the forms of transition curves that would be

most representative of high-speed railways. The basis for the identification of transition curves is the distribution of curvature κ over their length l [11, 16]. This distribution results from the boundary conditions imposed on the curvature at the initial and end sections. The function $\kappa(l)$ is determined from the corresponding differential equation.

The implementation of transition curves in the field requires the determination of their coordinates in the Cartesian coordinate system (x, y). This requires determining the slope of the tangent to the x-axis (assuming that it is zero at the starting point).

$$\Theta(l) = \int \kappa(l) dl \tag{4}$$

The transition curve is described by the following parametric equations:

$$x(l) = \int \cos\Theta(l) dl \tag{5}$$

$$y(l) = \int \sin\Theta(l) dl \tag{6}$$

whereby – in general terms – this requires the expansion of the sub-integral functions into a Taylor series [14] (in the case of transition curves, the Taylor series usually becomes a Maclaurin series).

A simplified method of determining the equation of the transition curve, leading to this equation in the form of an explicit function $y(x)$, is still in use on railways. The simplification of this procedure involves assuming that the modelled curvature $\kappa(l)$ relates to its projection on the x-axis, i.e. that $l = x$. This makes it possible to obtain the curvature equation $\kappa_0(x)$. However, it is impossible to determine the function $y(x)$ analytically, as this would require solving a differential equation.

$$\kappa_0(x) = \frac{y''(x)}{\left(\sqrt{1+\left[y'(x)\right]^2}\right)^3} \tag{7}$$

Therefore, $\kappa_0(x)$ is considered to be the equation of the second derivative of the sought function $y(x)$:

$$y''(x) \approx \kappa_0(x) \tag{8}$$

This equation is then integrated twice, providing $y'(x)$ and $y(x)$, given the conditions: $y(0) = 0$ and $y'(0) = 0$.

This is the course of action contained in such documents as the Technical Standards [21]. However, the use of these simplifications does not seem justified. Therefore, when selecting transition curves for the analysis carried out in this paper, the correct solution was adopted (i.e. in the form of parametric equations). Three cases of modelling boundary conditions were considered:

- the case of ensuring continuity of the curvature graph (concerning the clothoid),
- the case of smoothing of the curvature graph at the initial and end sections (concerning the Bloss curve),
- the case of smoothing of the curvature graph only at the end section (concerning the proposed new form of the curve).

4.1. Clothoid

The curvature of the clothoid [11] must satisfy two basic (i.e., continuity-ensuring) boundary conditions for the starting point (i.e., $l = 0$) and the end point (i.e., $l = l_k$):

$$\begin{cases} \kappa(0^+) = 0 \\ \kappa\left(l_k^-\right) = \dfrac{1}{R} \end{cases} \tag{9}$$

and the differential equation

$$\kappa''(l) = 0 \tag{10}$$

The solution of the differential problem (9), (10) is as follows:

$$\kappa(l) = \frac{1}{R \cdot l_k} l \tag{11}$$

i.e. this is the case of a linear change in curvature.

Expression (11), by integration, makes it possible to determine the equation of the angle $\Theta(l)$.

$$\Theta(l) = \frac{1}{2 \cdot R \cdot l_k} l^2 \tag{12}$$

and its final value:

$$\Theta(l_k) = \frac{l_k}{2 \cdot R} \tag{13}$$

The expansions of the functions cosΘ(*l*) and sinΘ(*l*) into the Maclaurin series are as follows:

$$\cos\Theta(l)=1-\frac{l^4}{8\cdot R^2\cdot l_k^2}+\frac{l^8}{384\cdot R^4\cdot l_k^4}-\frac{l^{12}}{46{,}080\cdot R^6\cdot l_k^6}+\\+\frac{l^{16}}{10{,}321{,}920\cdot R^8\cdot l_k^8}-\ldots$$

$$\sin\Theta(l)=\frac{l^2}{2\cdot R\cdot l_k}-\frac{l^6}{48\cdot R^3\cdot l_k^3}+\frac{l^{10}}{3{,}840\cdot R^5\cdot l_k^5}-\\+\frac{l^{14}}{645{,}120\cdot R^7\cdot l_k^7}+\frac{l^{18}}{185{,}794{,}560\cdot R^9\cdot l_k^9}-\ldots$$

Equations (5) and (6) make it possible to determine the parametric equations *x*(*l*) and *y*(*l*). However, as it turns out, for high-speed railways with very large radii of horizontal curves and lengths of transition curves, these equations can be greatly simplified by eliminating most of the expressions of the series. In computational practice, the clothoid equations for HSR take the following form:

$$x(l)=l-\frac{l^5}{40\cdot R^2\cdot l_k^2} \tag{14}$$

$$y(l)=\frac{l^3}{6\cdot R\cdot l_k} \tag{15}$$

4.2. Bloss curve

The curvature of the Bloss curve [11] satisfies additional conditions that result in smoothing the curvature graph at the initial and final sections:

$$\begin{cases}\kappa(0^+)=\kappa'(0^+)=0\\ \kappa\left(l_k^-\right)=\dfrac{1}{R}\\ \kappa'\left(l_k^-\right)=0\end{cases} \tag{16}$$

The following differential equation applies to it:

$$\kappa^{(4)}(l)=0 \tag{17}$$

After solving the problem (16), (17), the following curvature equation is obtained:

$$\kappa(l)=\frac{3}{R\cdot l_k^2}l^2-\frac{2}{R\cdot l_k^3}l^3 \tag{18}$$

Here we see a classic (symmetrical) case of nonlinear curvature change. The angle equation Θ(*l*) follows from expression (18):

$$\Theta(l)=\frac{1}{R\cdot l_k^2}l^3-\frac{1}{2\cdot R\cdot l_k^3}l^4 \tag{19}$$

As it turns out, its final value is described by equation (13).

The expansions of the functions cosΘ(*l*) and sinΘ(*l*) into the Maclaurin series are as follows:

$$\cos\Theta(l)=1-\frac{l^6}{2\cdot R^2\cdot l_k^4}+\frac{l^7}{2\cdot R^2\cdot l_k^5}-\frac{l^8}{8\cdot R^2\cdot l_k^6}+\\+\frac{l^{12}}{24\cdot R^4\cdot l_k^8}-\frac{l^{13}}{12\cdot R^4\cdot l_k^9}+\ldots$$

$$\sin\Theta(l)=\frac{l^3}{R\cdot l_k^2}-\frac{l^4}{2\cdot R\cdot l_k^3}-\frac{l^9}{6\cdot R^3\cdot l_k^6}+\\+\frac{l^{10}}{4\cdot R^3\cdot l_k^7}-\frac{l^{11}}{8\cdot R^3\cdot l_k^8}+\frac{l^{12}}{48\cdot R^3\cdot l_k^9}+\ldots$$

After integration (and elimination of irrelevant expressions from the sequence), the parametric equations of the Bloss curve are obtained, adapted to HSR computational practice:

$$x(l)=l-\frac{l^7}{14\cdot R^2\cdot l_k^4}+\frac{l^8}{16\cdot R^2\cdot l_k^5}-\frac{l^9}{72\cdot R^2\cdot l_k^6} \tag{20}$$

$$y(l)=\frac{l^4}{4\cdot R\cdot l_k^2}-\frac{l^5}{10\cdot R\cdot l_k^3}-\frac{l^{10}}{60\cdot R^3\cdot l_k^6}+\\+\frac{l^{11}}{44\cdot R^3\cdot l_k^7}-\frac{l^{12}}{96\cdot R^3\cdot l_k^8} \tag{21}$$

4.3. New transition curve

Guided by performance practice, the author of this paper has proposed a transition curve which, unlike the Bloss curve, has a smoothed curvature only at the end section. This curve satisfies the boundary conditions set out below [12]:

$$\begin{cases} \kappa(0^+) = 0 & \kappa\left(l_k^-\right) = \dfrac{1}{R} \\ \kappa'\left(0^+\right) = \dfrac{1}{R \cdot l_k} & \kappa'\left(l_k^-\right) = 0 \end{cases} \tag{22}$$

and the differential equation (17). After solving the problem (17), (22), the following curvature equation is obtained:

$$\kappa(l) = \frac{1}{R \cdot l_k} l + \frac{1}{R \cdot l_k^2} l^2 - \frac{1}{R \cdot l_k^3} l^3 \tag{23}$$

Condition (4) makes it possible to determine the equation of the angle $\Theta(l)$:

$$\Theta(l) = \frac{1}{2 \cdot R \cdot l_k} l^2 + \frac{1}{3 \cdot R \cdot l_k^2} l^3 - \frac{1}{4 \cdot R \cdot l_k^3} l^4 \tag{24}$$

and its final value:

$$\Theta(l_k) = \frac{7}{12 \cdot R} l_k \tag{25}$$

The expansions of the functions $\cos\Theta(l)$ and $\sin\Theta(l)$ into the Maclaurin series are as follows:

$$\cos\Theta(l) = 1 - \frac{l^4}{8 \cdot R^2 \cdot l_k^2} - \frac{l^5}{6 \cdot R^2 \cdot l_k^3} + \frac{5 \cdot l^6}{72 \cdot R^2 \cdot l_k^4} + \frac{l^7}{12 \cdot R^2 \cdot l_k^5} + \frac{l^8}{384 \cdot R^4 \cdot l_k^4} - \frac{l^8}{32 \cdot R^2 \cdot l_k^6} - \ldots$$

$$\sin\Theta(l) = \frac{l^2}{2 \cdot R \cdot l_k} + \frac{l^3}{3 \cdot R \cdot l_k^2} - \frac{l^4}{4 \cdot R \cdot l_k^3} - \frac{l^6}{48 \cdot R^3 \cdot l_k^3} - \frac{l^7}{24 \cdot R^3 \cdot l_k^4} + \frac{l^8}{288 \cdot R^3 \cdot l_k^5} - \ldots$$

After integration, parametric equations for the new transition curve are obtained, adapted to the HSR calculation practice:

$$x(l) = l - \frac{l^5}{40 \cdot R^2 \cdot l_k^2} - \frac{l^6}{36 \cdot R^2 \cdot l_k^3} + \frac{5 \cdot l^7}{504 \cdot R^2 \cdot l_k^4} + \frac{l^8}{96 \cdot R^2 \cdot l_k^5} + \frac{l^9}{3,456 \cdot R^4 \cdot l_k^4} - \frac{l^9}{288 \cdot R^2 \cdot l_k^6} \tag{26}$$

$$y(l) = \frac{l^3}{6 \cdot R \cdot l_k} + \frac{l^4}{12 \cdot R \cdot l_k^2} - \frac{l^5}{20 \cdot R \cdot l_k^3} + \frac{l^7}{336 \cdot R^3 \cdot l_k^3} - \frac{l^8}{192 \cdot R^3 \cdot l_k^4} \tag{27}$$

5. Test geometric layouts

5.1. Determination of test layout parameters

Guided by principles set out in items 2 and 3, the parameters of the test geometric layouts, which were the subject of comparative analysis, were determined. It was assumed that these layouts would be symmetrical, characterised by the same length of both transition curves. A train speed of V = 350 km/h and a cant value on the curve of D_0 = 120 mm were assumed, giving a radius of R_{min} = 6,600 m. The corresponding minimum length of the clothoid transition curve is l_{min} = 234 m. For the test layout, a radius value of R = 7,500 m and a clothoid length of l_k = 250 m were assumed. The curve deflection angle was also determined, assuming a value of $\alpha = \pi/3$ rad. To be able to compare individual geometric systems, the use of the other two types of transition curves requires a corresponding increase in their length. This is due to the need to maintain acceptable values of the kinematic parameters. As the ratio of the length of the Bloss curve to the length of the clothoid is 1.5 [11], l_k = 375 m should be assumed for it in the test layout. In contrast, the length of the new curve must be 1/3 longer than that of the clothoid [12], so a value of l_k = 335 m was adopted.

5.2. Curvature graphs for the lengths of the transition curves

The test geometric layouts under consideration differ in terms of the type of transition curves used. The corresponding curvature graphs for the lengths of these curves are shown in Figure 3.

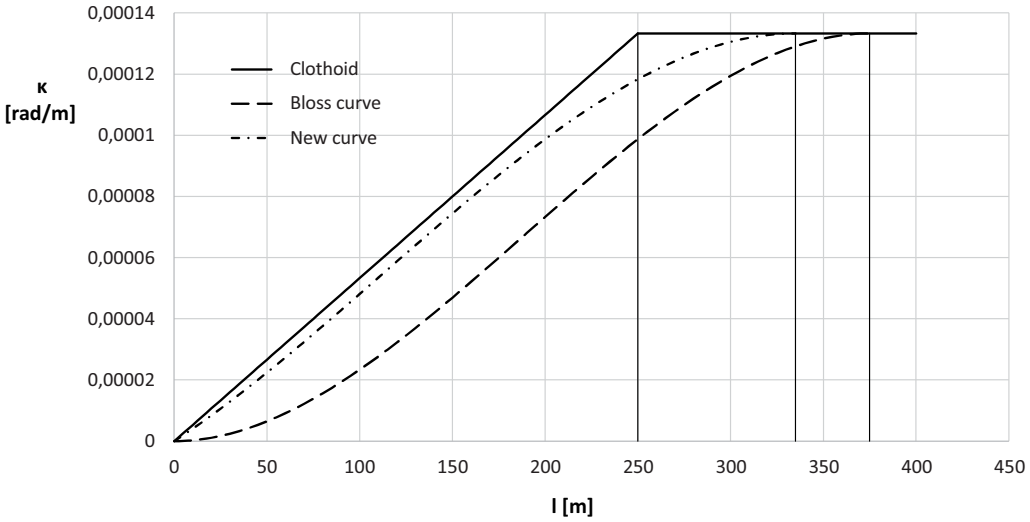

Fig. 3. Curvature graphs for the lengths of the applied transition curves [author's own elaboration]

As can be seen, the curvature graphs for the clothoid and the new transition curve are similar to each other at the initial section. However, a clear difference is revealed at the end section, where the new curve provides a smooth entry into the circular curve. The Bloss curve is characterised by a softening of the curvature at both the initial and end sections. It should also be noted that the dynamic analysis carried out in [10] confirms that the new transition curve is slightly more favourable than the clothoid at the initial section and has a clear advantage over it at the end section (which results from the boundary conditions adopted when determining the curvature equation). Indeed, the superiority of the new curve over the Bloss curve at the end section was demonstrated as well.

5.3. Test layouts in the Cartesian coordinate system

Designing track geometrical layouts consists in determining their Cartesian coordinates in the national spatial reference system. In Poland – with regard to plane coordinates – the PL-2000 system is in force [19]. In the analytical design method [13], the relevant calculations are carried out using the local x, y coordinate system. The beginning of this layout is located at the intersection of adjacent main route directions (marked W). For a symmetrical alignment of the main directions, a transformation (shifting and rotation) of the PL-2000 system coordinates is required. The system's starting point is shifted to point W, while rotation takes place with respect to this point by an angle β, until a symmetrical alignment of lines i and $i+1$ is achieved (Fig. 4).

Figure 4 uses the following designations: W – intersection point of the main directions, the starting point of the local coordinate system; P – the starting point of the designed layout; K_1 – the end of the first transition curve; S – the centre of the horizontal arc, K_2 – the end of the second transition curve, K – the end of the designed system.

Using the design methodology described in paper [13], three test layouts were obtained for the different types of transition curves used. Figure 5 shows a portion of the area where the straight section on the left side of the route is connected to the horizontal curve

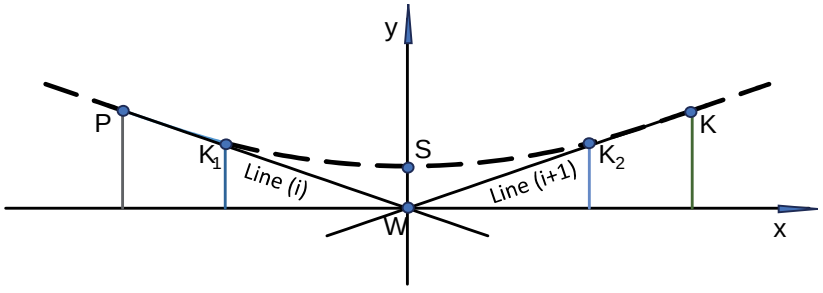

Fig. 4. Conceptual symmetrical geometric layout in the local coordinate system [author's own elaboration]

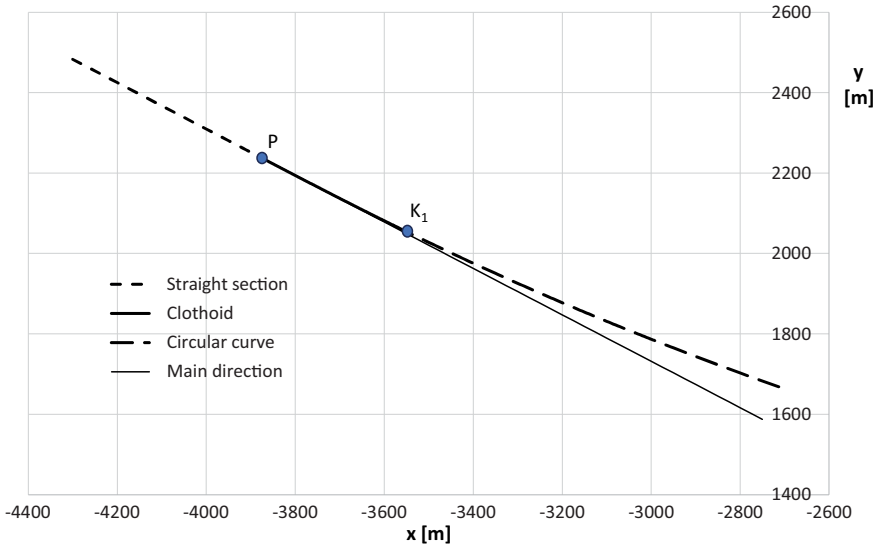

Fig. 5. Fragment of the test layout – the connection of the straight line with the horizontal curve by means of a clothoid transition curve [author's own elaboration]

Table 1

Summary of the Cartesian system coordinates for the test layouts under consideration

Transition curve	Abscissa x_P [m]	Ordinate y_P [m]	Abscissa x_{KI} [m]	Ordinate y_{KI} [m]	Abscissa x_S [m]	Ordinate y_S [m]
Clothoid	–3,858.426	2,227.663	–3,641.231	2,103.869	0	1,160.655
Bloss curve	–3,912.613	2,258.948	–3,586.465	2,073.894	0	1,160.795
New curve	–3,871.104	2,234.983	–3,579.511	2,070.087	0	1,160.770

[Authors' own elaboration].

by means of a clothoid transition curve. For the other curves, geometric layouts were obtained that visually – at the adopted graph scale – differed basically only in the location of the P and K_1 points. A summary of the corresponding numerical values for half of the test layout is given in Table 1 (the other half of the system is symmetrical).

Particularly noteworthy are the ordinate values at the centre point of the horizontal curve. They are very close to each other, and this is no coincidence. As it turns out, in the range $\langle -3{,}579.511; 3{,}579.511 \rangle$ m, covering horizontal curves in all test layouts, the circular curve of the Bloss curve layout is shifted upwards (i.e., towards its centre) by only 140 mm compared to the clothoid layout. In contrast, the circular curve of the system with the new transition curve is shifted relative to the clothoid system (also upwards) by 115 mm. Thus, the test layouts considered virtually overlap along their entire lengths.

However, it is worth considering one more point, namely the formation of the horizontal ordinates at the initial sections of the respective transition curves. This is shown in Table 2 for the initial 50 m section, with the relevant main route direction (i.e., the tangent to the transition curve at its starting point) used as a reference. The ordinate values were given to the nearest 0.001 mm, which, of course, does not meet the requirements of performance practice, but was relevant to the comparative analysis carried out. The corresponding graphs are shown in Figure 6.

As can be seen, the ordinates of the transition curve at the initial section are very small in all cases considered. It is difficult to say whether the existing implementation capabilities (i.e., the accuracy currently achieved) will enable an appropriate horizontal shape of a given curve. While there is a chance for this in the case of the clothoid and the new curve, it does not seem possible in the case of the Bloss curve. After the first 30 m, the horizontal ordinate for the Bloss curve is 0.2 mm, and after 50 m, it is less than 1.5 mm. Such a geometric layout cannot be set up in field conditions. In practice, this would mean a significant shortening of the transition curve.

The last remark also applies to other smooth transition curves (such as cosine and sine). And it is precisely these curves, with gentle curvature graphs

Table 2

Ordinates of the transition curve at the initial section (in relation to the main direction of the route)

Coordinate l [m]	Clothoid y_k [mm]	Bloss curve y_k [mm]	New curve y_k [mm]
0	0.000	0.000	0.000
2	0.000	0.000	0.001
4	0.002	0.000	0.004
6	0.019	0.000	0.014
8	0.046	0.001	0.034
10	0.089	0.002	0.067
12	0.154	0.005	0.117
14	0.244	0.009	0.186
16	0.364	0.015	0.278
18	0.518	0.024	0.397
20	0.711	0.037	0.546
22	0.946	0.054	0.729
24	1.229	0.077	0.948
26	1.562	0.105	1.209
28	1.951	0.141	1.514
30	2.400	0.186	1.867
32	2.913	0.240	2.272
34	3.494	0.305	2.731
36	4.147	0.383	3.250
38	4.878	0.474	3.832
40	5.689	0.581	4.481
42	6.586	0.705	5.200
44	7.572	0.847	5.993
46	8.652	1.009	6.864
48	9.830	1.194	7.817
50	11.111	1.402	8.855

[Authors' own elaboration].

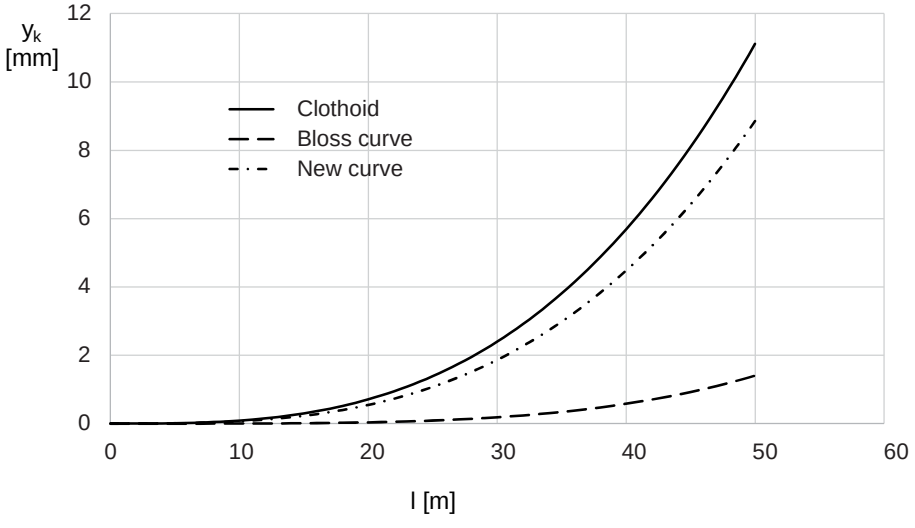

Fig. 6. Graphs of ordinates of the transition curve at the initial section in relation to the main direction of the route [author's own elaboration]

at their extreme points, that are most advantageous from a theoretical point of view (i.e. the occurring dynamic interactions) [10]. Still, performance practice highlights other aspects of the issue at hand. Doubts about the effective applicability of smooth transition curves on traditional railways were formulated in such papers as [12] and formed the basis for the development of a new form of curve. On high-speed railways, these constraints may be multiplied by the much larger radii of horizontal curves and lengths of transition curves adopted.

After selecting the most advantageous transition curve, two other curves remain to be considered and their curvature has not been smoothed at the starting point. Paper [10] shows that the proposed new curve is significantly more favourable than the clothoid curve from the point of view of dynamic interactions. Yet, issues related to the possibilities of effectively shaping gradients due to cant still needed to be investigated.

6. Shaping of gradients due to cant

The gradients due to cant serves to balance lateral acceleration along the length of the transition curve. As this acceleration results from the curvature of the track axis, the change in cant over the length of the gradients due to cant must correspond to the change in curvature. Hence the need to maintain proportionality between the ordinates of the gradients due to cant and the corresponding values of the curvature. Figure 7 shows graphs of gradients due to cant ordinates for the lengths of the transition curves used.

As can be seen, the shapes of the graphs in Figure 7 fully correspond to the curvature graphs in Figure 3. Moreover, for the Bloss curve – like for the ordinates of this curve in Figure 6 – the values of the gradients due to cant ordinates at the initial section are very small. Indeed, they are impossible to implement and subsequently maintain from a practical standpoint. This is shown numerically in Table 3 and graphically in Figure 8 for the initial 50 m section. The ordinate values in Table 3, like the horizontal ordinates in Table 2, were given to the nearest 0.001 mm, which was important from the point of view of the comparative analysis carried out.

As it turns out, the gradient due to cant cant ramp ordinate on the Bloss curve is less than 0.1 mm for l = 5 m, 0.25 mm for l = 10 m, 0.56 mm for l = 15 m and 1 mm for l = 20 m. This is in no way achievable under actual operating conditions, and the gradient due to cant will simply be shortened. The gradient due to cant on the new curve is completely different. Its ordinates amount to 75–80% of those of the clothoid gradient due to cant and this percentage increases with the length of the curve.

The above leads to an obvious conclusion: the Bloss curve, like other smooth transition curves (with smoothed curvature at the initial section), is unsuitable for high-speed railway conditions due to the difficulties in shaping it correctly at the initial section; this applies to both the horizontal plane and the gradient due to cant. These conditions are undoubtedly fulfilled by a clothoid transition curve. However, it is worth considering whether it would be more beneficial to use the transition curve described by parametric equations (26) and (27), which provides a smoother transition to the horizontal curve from the point of view of both the occurring curvature and the shape of the gradient due to cant.

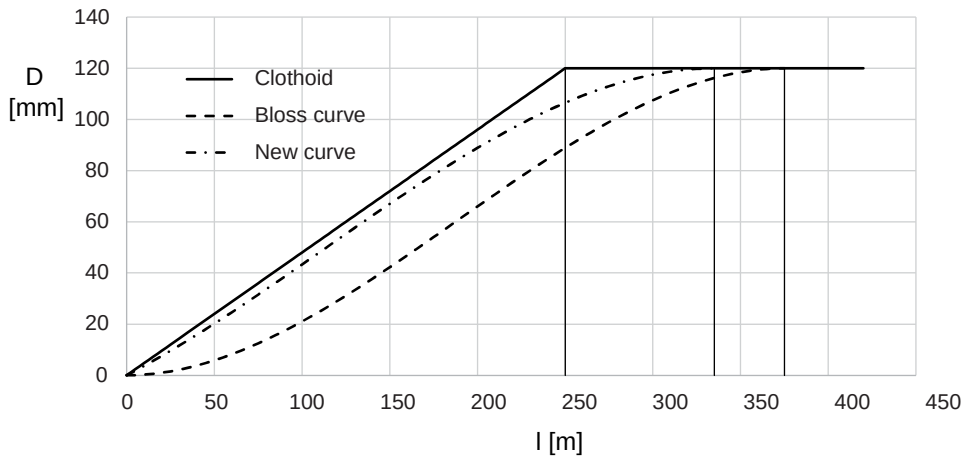

Fig. 7. Graphs of gradients due to cant ordinates for the lengths of the transition curves used [author's own elaboration]

Table 3

Gradients due to cant ordinates at the initial section of the test layouts under consideration

Coordinate *l* [m]	Clothoid *D* [mm]	Bloss curve *D* [mm]	New curve *D* [mm]
0	0.000	0.000	0.000
2	0.960	0.010	0.721
4	1.920	0.041	1.450
6	2.880	0.091	2.187
8	3.840	0.162	2.932
10	4.800	0.251	3.686
12	5.760	0.361	4.447
14	6.720	0.489	5.216
16	7.680	0.637	5.992
18	8.640	0.803	6.776
20	9.600	0.988	7.566
22	10.560	1.191	8.364
24	11.520	1.412	9.169
26	12.480	1.651	9.980
28	13.440	1.907	10.798
30	14.400	2.181	11.622
32	15.360	2.472	12.453
34	16.320	2.780	13.290
36	17.280	3.105	14.132
38	18.240	3.447	14.981
40	19.200	3.805	15.835
42	20.160	4.179	16.695
44	21.120	4.568	17.559
46	22.080	4.974	18.430
48	23.040	5.395	19.305
50	24.000	5.831	20.185

[Authors' own elaboration].

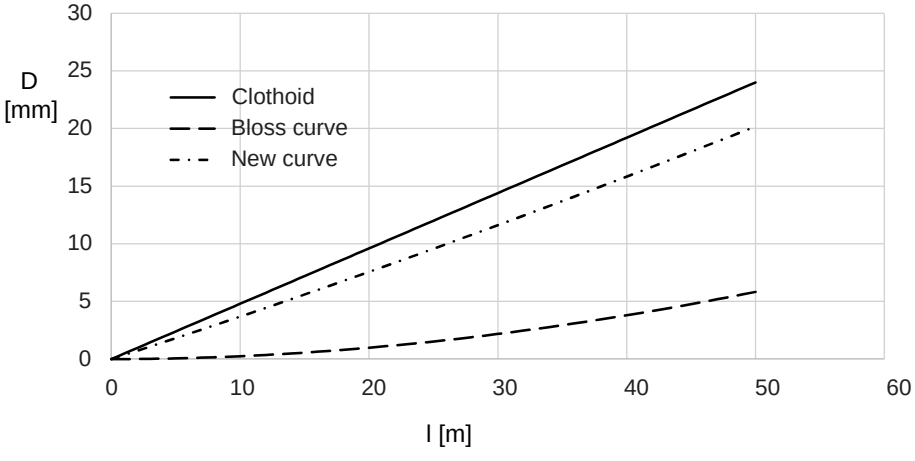

Fig. 8. Graphs of gradient due to cant ordinates for the initial 50 m of the transition curves used [author's own elaboration]

7. Conclusions

The European Union's Technical Specifications for Interoperability relating to the "Infrastructure" subsystem introduce certain modifications – sometimes quite significant ones. It seems worthwhile to examine what impact the new conditions have had on the design process of track geometric layouts. This mainly concerns the accepted limit values for kinematic parameters. Particular attention should be given to those issues that are dealt with in a limited way in the TSI. This is precisely the case with transition curves, for which the new design rules leave considerable discretion. It seems that the resolution of this issue has been left to national regulations.

This article proposes – based on the applicable EU and national rules – acceptable values for the kinematic parameters that should correspond to the design of transition curves. A number of cases were considered for different speeds between 250 and 350 km/h and cant ranging from 60 mm to 180 mm. Minimum values for the radii of horizontal arcs and the lengths of transition curves were determined, depending on train speed and cant on the arc. The transition curves that would be most representative from the point of view of high-speed railways were then selected. The basis for identifying the curves was the distribution of curvature along their length. Three forms of transition curves were considered: a clothoid curve (ensuring continuity of the curvature graph), a Bloss curve (with smoothed curvature at the initial and end sections) and a new transition curve described by parametric equations (26) and (27) (with smoothed curvature only at the end section).

Guided by previously established principles, the parameters of the test geometric layouts, which were the subject of comparative analysis, were determined. This analysis showed that, in the horizontal plane, the test layouts nearly overlapped along their entire lengths. One could therefore conclude that the type of transition curve does not pose any special implementation issues for high-speed railways. However, this is not the case, as there are issues with shaping the horizontal ordinates of smooth transition curves (such as the Bloss curve) at the initial section. In the latter case, the shape of the curve differs little from a straight line (i.e. the main direction of the route) and it is impossible to form the correct geometrical layout in field conditions. Similar problems arise with respect to the shaping of the gradient due to cant. For the Bloss curve, the values of the gradient due to cant ordinates at the initial section are very small. Indeed, they are impossible to implement and subsequently maintain from a practical standpoint.

Doubts about the applicability of smooth transition curves on traditional railways were formulated in such papers as [12] and formed the basis for the development of a new form of curve. On high-speed railways, the constraints of shaping the initial section of these curves (both in terms of the horizontal plane and their gradient due to cant may be multiplied by the much larger radii of horizontal curves and lengths of transition curves adopted. Therefore, the curves in question do not correspond to the conditions found on high-speed railways. These conditions are undoubtedly met by a clothoid transition curve, but the curve described by parametric equations (26) and (27) seems to be more advantageous, as it provides a smoother transition to a circular curve on its end section.

References

1. Bałuch M.: *Selection of kinematic parameter values in the design of railway line modernization* (in Polish), Problemy Kolejnictwa – Railway Reports, issue 119/1995, pp. 54–70, Wydawnictwo Centrum Naukowo-Technicznego Kolejnictwa.
2. Commission Decision of 20 December 2007 concerning a technical specification for interoperability relating to the 'infrastructure' subsystem of the trans-European high speed rail system, Official Journal of the European Union, L 77/1, Vol. 51, 19 January 2008, Publications Office of the EU, Luxembourg.
3. Commission Decision of 26 April 2011 concerning a technical specification for interoperability relating to the 'infrastructure' subsystem of the trans-European conventional rail system, Official Journal of the European Union, L 126/53, Vol. 54, 14 May 2011, Publications Office of the EU, Luxembourg.
4. Commission regulation (EU) No 1299/2014 of 18 November 2014 on the technical specifications for interoperability relating to the 'infrastructure' subsystem of the rail system in the European Union, Official Journal of the European Union, L 356/1, Vol. 57, 12 December 2014, Publications Office of the EU, Luxembourg.
5. Commission Regulation (EU) No 1302/2014 of 18 November 2014 concerning a technical specification for interoperability relating to the 'rolling stock – locomotives and passenger rolling stock' subsystem of the rail system in the European Union, Official Journal of the European Union, L 356/228, Vol. 57, 12 December 2014, Publications Office of the EU, Luxembourg.
6. Esveld C.: *Developments in high-speed track design,* IABSE Symposium Report, No. 12/2003, pp. 37–45, Science Gate.
7. Guerrieri M.: *Fundamentals of railway design*, *Chapter: The alignment design of ordinary and high-speed railways*, Springer, 2023, pp. 21–56.

8. High–speed rail in Poland. Advances and perspectives, Editor: A. Żurkowski, Railway Research Institute in Warsaw, CRS Press, London, UK, 2018.
9. Hodas S.: *Design of ailway track for speed and high-speed railways*, Procedia Engineering, Vol. 91/2014, pp. 256–261, Elsevier.
10. Koc W., Palikowska K.: *Assessment of dynamic properties and scope of implementing a new track transition curve*, Journal of Surveying Engineering, No. 1/2021, article ID: 04020022, American Society of Civil Engineers.
11. Koc W.: *Identification of transition curves in vehicular roads and railways*. Logistics and Transport, No. 4/2015, pp. 31–42, The International University of Logistics and Transport in Wrocław.
12. Koc W.: *New transition curve adapted to railway operational requirements*, Journal of Surveying Engineering, No. 3/2019, article ID: 04019009, American Society of Civil Engineers.
13. Koc W.: *Basic variants of the analytical method of designing track geometric layouts,* Problemy Kolejnictwa – Railway Reports, issue 200/2023, pp. 171–185, Wydawnictwo Instytutu Kolejnictwa.
14. Korn G.A., Korn T.M.: *Mathematical handbook for scientists and engineers*, 1st ed., McGraw–Hill Book Company: New York, USA, 1968.
15. Liu X., Zhao P., Dai F.: *Advances in design theories of high-speed railway ballastless tracks*, Journal of Modern Transportation, No. 3/2011, pp. 154–162, Springer Professional.
16. Mieloszyk E., Koc W.: *General dynamic method for determining transition curve equations*, Rail International – Schienen der Welt, No. 10/1991, pp. 32–40.
17. Raif L. et.al.: *Design of high-speed turnouts and crossings*, IOP Conference Series: Materials Science and Engineering, No. 1/2017, pp. 1–7, IOP-science.
18. Regulation of the Minister of Transport and Maritime Economy of 10 September 1998 on technical conditions to be met by railway structures and their location (in Polish), Dz.U. /Journal of Laws/ of 1998, No. 151, item 987.
19. Regulation of the Council of Ministers of 15 October 2012 on the state system of spatial references (consolidated text) (in Polish), Dz.U. /Journal of Laws/ of 2024, item 342.
20. Technical Standards – detailed technical conditions for the modernization or construction of railway lines up to a speed of $V_{max} \leq 200$ km/h (for conventional rolling stock) / 250 km/h (for tilting rolling stock) (in Polish), PKP Polish Railway Lines S.A., Warszawa, 2009.
21. Technical Standards – detailed technical conditions for the modernization or construction of railway lines up to a speed of $V_{max} \leq 250$ km/h. Volume I – Railroad – Appendix ST-T1-A6 – Geometric layouts of tracks (in Polish), PKP Polish Railway Lines S.A., Warszawa 2021.
22. Wang J.: *Safety theory and control technology of high-speed train operation*, Academic Press, Published by Elsevier Inc., 2018.
23. Wang P.: *Design of high-speed railway turnouts. Theory and applications*, Academic Press, Published by Elsevier Inc., 2015.
24. Yi S.: *High-speed railway alignment. Thery and practice*, Academic Press, Published by Elsevier Inc., 2018.
25. Yi S.: *Principles of railway location and design*, Academic Press, Published by Elsevier Inc., 2018.